

Comprehensive Analysis of the Neglect of Diatomic Differential Overlap Approximation

Tamara Husch and Markus Reiher*

ETH Zürich, Laboratorium für Physikalische Chemie,
Vladimir-Prelog-Weg 2, 8093 Zürich, Switzerland.

April 7, 2024

Abstract

Many modern semiempirical molecular orbital models are built on the neglect of diatomic differential overlap (NDDO) approximation. An in-depth understanding of this approximation is therefore indispensable to rationalize the success of these semiempirical molecular orbital models and to develop further improvements on them. The NDDO approximation provides a recipe to approximate electron-electron repulsion integrals (ERIs) in a symmetrically orthogonalized basis based on a far smaller number of ERIs in a locally orthogonalized basis. We first analyze the NDDO approximation by comparing ERIs in both bases for a selection of molecules and for a selection of basis sets. We find that the errors in Hartree–Fock and second-order Møller–Plesset perturbation theory energies grow roughly linearly with the number of basis functions. We then examine different approaches to correct for the errors caused by the NDDO approximation and propose a strategy to directly correct for them in the two-electron matrices that enter the Fock operator.

*corresponding author: markus.reiher@phys.chem.ethz.ch.

1 Introduction

The neglect of diatomic differential overlap (NDDO) approximation¹ is the foundation of the MNDO model² and is therefore passed on to modern semiempirical molecular orbital (SEMO) models such as AM1,³ PM x ($x = 3, 6, 7$),⁴⁻⁶ and OM x ($x = 1, 2, 3$).⁷⁻⁹ These SEMO models are chosen when, on the one hand, accurate *ab initio* electronic structure models are computationally unfeasible — but when, on the other hand, a calculation with an electronic structure model is favored over a classical force field to exploit the first-principles nature of the fundamental electrostatic interactions. Examples include the simulation of very large systems such as proteins,¹⁰⁻¹⁷ virtual high-throughput screening schemes for materials and drug discovery,¹⁸⁻²⁵ or real-time interactive quantum chemical calculations.²⁶⁻³²

Originally, the NDDO approximation was conceptualized as a means to reduce the number of electron-electron repulsion integrals (ERIs) that need to be explicitly calculated in the course of a Hartree–Fock (HF) calculation.¹ The NDDO approximation specifies how ERIs in a symmetrically orthogonalized basis may be approximated based on a far smaller number of ERIs in a locally orthogonalized basis. However, the NDDO approximation has not found acceptance in *ab initio* calculations due to the significant errors that it introduced in ERIs in the symmetrically orthogonalized basis.³³⁻⁵¹ Instead, the NDDO approximation has become popular in SEMO models where it is combined²⁻⁹ with various other approximations made to the ERIs, to the one-electron matrix, and to the nucleus-nucleus repulsion energy which benefit from mutual error compensation. We refer to Ref. 52 for a comprehensive summary of all approximations incorporated in popular NDDO-SEMO models. An important approximation to highlight in this context is the empirical modification of the ERIs in NDDO-SEMO models²⁻⁹ where the ERIs are scaled so that they are usually significantly smaller than the analytically calculated ones. This scaling then compensates other approximations in SEMO models. The results obtained with *ab initio* electronic structure models invoking the NDDO approximation can therefore not be directly related to results obtained with modern NDDO-SEMO models. Nevertheless, an in-

depth analysis of the NDDO approximation is mandatory to develop further improvements to NDDO-SEMO models. Despite decades of work on NDDO-SEMO models, a fully satisfactory analysis has not been provided yet. We intend to take a step toward closing this gap here and study the foundations of the NDDO approximation from a state-of-the-art perspective.

First, we determine how the NDDO approximation affects ERIs evaluated in a symmetrically orthogonalized basis. Previous analyses of the NDDO approximation were limited to few tens of molecules that consisted of a few atoms (usually less than four heavy atoms).^{34–51} In this work, we consider a diverse selection of molecules that are also much larger. As the errors in the ERIs will propagate to all quantities calculated in an NDDO framework, we study how the NDDO approximation affects the (absolute and relative) HF and second-order Møller–Plesset perturbation (MP2) theory energies. In this context, we examine different basis set choices.

In general, the NDDO approximation is only valid for a locally orthogonal basis set,^{46–48,50} which appears to restrict contemporary NDDO-SEMO models to a minimal basis set. A minimal basis set, however, is generally unsuitable for the description of atoms in molecules because it does not yield reliable relative energies, force constants, electric dipole moments, static dipole polarizabilities, and other properties.^{53–58} It was suggested to generalize NDDO-SEMO models to larger, e.g., double-zeta split-valence basis sets to obtain more accurate results.⁵⁹ Two studies examined^{60,61} the effects of the application of a double-zeta split-valence basis set in conjunction with the NDDO approximation, but came to the conclusion that, contrary to what one would expect, the results did not improve compared to the results obtained with a single-zeta basis set. In this work, we dissect in detail the origins of this counterintuitive observation.

It does not come as a surprise that we find — in agreement with previous results^{34–51} — the NDDO approximation to cause severe errors. We therefore examine how one can correct for these errors. We briefly review the error compensation strategy that contemporary NDDO-SEMO models apply and then propose a way to directly correct for errors in the two-electron matrices. We show that our approach allows for rapid calculations invoking the NDDO

approximation with error control.

2 Neglect of Diatomic Differential Overlap Approximation

2.1 Basic Notation

In a basis-set representation, each spatial molecular orbital $\psi_i = \psi_i(\mathbf{r})$ is approximated as a linear combination of pre-defined basis functions. Following the well-established approach for finite systems in molecular physics, we choose the basis functions to be Gaussian-type atom-centered functions $\chi_\mu^I = \chi_\mu^I(\mathbf{r})$. Our notation indicates that the μ -th basis function of type χ is centered on atom I . Additionally, we require the basis functions χ to be locally orthogonal which means that the overlap ${}^xS_{\mu\nu}$ between the basis functions χ_μ^I and χ_ν^J must fulfill,

$${}^xS_{\mu\nu} = \begin{cases} \langle \chi_\mu^I | \chi_\nu^J \rangle & I \neq J, \forall \mu, \nu \\ \delta_{\mu\nu} & I = J, \forall \mu, \nu \end{cases}, \quad (1)$$

where $\delta_{\mu\nu}$ is the Kronecker delta. A molecular orbital ψ_i is then given as the sum of the M basis functions χ_μ^I weighted with expansion coefficients ${}^x\mathbf{C} = \{{}^xC_{\mu i}\}$,

$$\psi_i(\mathbf{r}) = \sum_{\mu=1}^M {}^xC_{\mu i} \chi_\mu^I(\mathbf{r}). \quad (2)$$

Throughout this work, we denote the bases by a left superscript, i.e., ${}^x\mathbf{C}$. In the χ -basis, the Roothaan–Hall equation in the spin-restricted formulation then reads⁵⁴

$${}^x\mathbf{F}({}^x\mathbf{C}) {}^x\mathbf{C} = {}^x\mathbf{S} {}^x\mathbf{C} \boldsymbol{\epsilon}, \quad (3)$$

where ${}^x\mathbf{F}$ is the Fock matrix, which depends on ${}^x\mathbf{C}$, ${}^x\mathbf{S}$ is the overlap matrix, and $\boldsymbol{\epsilon}$ is the diagonal matrix of orbital energies. As $\boldsymbol{\epsilon}$ is invariant under unitary matrix transformations with which we may transform one basis into

another one, it does not carry a left superscript. The evaluation of the Fock-matrix elements in the χ -basis,⁵⁴

$${}^x F_{\mu\nu}({}^x \mathbf{C}) = \langle \chi_\mu^I | h | \chi_\nu^J \rangle + \sum_{\lambda\sigma} {}^x P_{\lambda\sigma}({}^x \mathbf{C}) \left[\langle \chi_\mu^I \chi_\nu^J | \chi_\lambda^K \chi_\sigma^L \rangle - \frac{1}{2} \langle \chi_\mu^I \chi_\sigma^L | \chi_\lambda^K \chi_\nu^J \rangle \right], \quad (4)$$

requires the evaluation of one-electron integrals $\langle \chi_\mu^I | h | \chi_\nu^J \rangle$, elements of the density matrix ${}^x \mathbf{P}({}^x \mathbf{C})$, and ERIs in the χ -basis (x ERIs). In a spin-restricted framework, the elements of ${}^x \mathbf{P}({}^x \mathbf{C})$ are given by

$${}^x P_{\mu\nu}({}^x \mathbf{C}) = 2 \sum_{i=1}^{n/2} {}^x C_{\mu i} {}^x C_{\nu i}, \quad (5)$$

where n is the number of electrons, and the x ERIs are calculated according to

$$\langle \chi_\mu^I \chi_\nu^J | \chi_\lambda^K \chi_\sigma^L \rangle = \int \int \chi_\mu^{*,I}(\mathbf{r}_1) \chi_\nu^J(\mathbf{r}_1) \frac{1}{|\mathbf{r}_1 - \mathbf{r}_2|} \chi_\lambda^{*,K}(\mathbf{r}_2) \chi_\sigma^L(\mathbf{r}_2) d^3 r_1 d^3 r_2. \quad (6)$$

For the following discussion, it is convenient to divide the Fock matrix into a one-electron matrix ${}^x \mathbf{H}$ and a two-electron matrix ${}^x \mathbf{G}({}^x \mathbf{C})$ which, in HF theory, consists of a Coulomb matrix ${}^x \mathbf{J}({}^x \mathbf{C})$ and an exchange matrix ${}^x \mathbf{K}({}^x \mathbf{C})$,

$${}^x \mathbf{F}({}^x \mathbf{C}) = {}^x \mathbf{H} + {}^x \mathbf{G}({}^x \mathbf{C}) = {}^x \mathbf{H} + {}^x \mathbf{J}({}^x \mathbf{C}) + {}^x \mathbf{K}({}^x \mathbf{C}). \quad (7)$$

After reaching self-consistency, the total electronic HF energy of the system is calculated from ${}^x \mathbf{P}({}^x \mathbf{C})$, ${}^x \mathbf{F}({}^x \mathbf{C})$, and the nucleus-nucleus repulsion energy V ,

$$E_{\text{el}}^{\text{HF}}({}^x \mathbf{C}) = \frac{1}{2} \sum_{\mu\nu} {}^x P_{\nu\mu}({}^x \mathbf{C}) (2 {}^x H_{\mu\nu} + {}^x G_{\mu\nu}({}^x \mathbf{C})) + V. \quad (8)$$

We need to introduce a second basis, the symmetrically orthogonalized⁶² basis ϕ , to discuss the NDDO approximation. The symmetrically orthogonalized basis functions $\phi = \{\phi_\mu\}$ and the locally orthogonal basis functions $\chi = \{\chi_\mu^I\}$ are related through

$$\phi_\nu = \sum_{\mu=1}^M ({}^x S^{-\frac{1}{2}})_{\mu\nu} \chi_\mu^I. \quad (9)$$

Consequently, we can calculate the ERIs in the ϕ -basis ($^\phi$ ERIs) by a transformation involving the x ERIs,

$$\langle \phi_\mu \phi_\nu | \phi_\lambda \phi_\sigma \rangle = \sum_{\mu' \nu' \lambda' \sigma'}^M ({}^x S^{-\frac{1}{2}})_{\mu\mu'} ({}^x S^{-\frac{1}{2}})_{\nu\nu'} \langle \chi_{\mu'}^I \chi_{\nu'}^J | \chi_{\lambda'}^K \chi_{\sigma'}^L \rangle ({}^x S^{-\frac{1}{2}})_{\lambda\lambda'} ({}^x S^{-\frac{1}{2}})_{\sigma\sigma'}. \quad (10)$$

This is formally a 4-index transformation which scales as $\mathcal{O}(M^5)$.⁵⁵

2.2 Definition of the Approximation

The NDDO approximation provides a recipe for how to estimate $^\phi$ ERIs based on a small number of x ERIs,¹

$$\langle \phi_\mu \phi_\nu | \phi_\lambda \phi_\sigma \rangle \approx \delta_{IJ} \delta_{KL} \langle \chi_\mu^I \chi_\nu^J | \chi_\lambda^K \chi_\sigma^L \rangle. \quad (11)$$

As a consequence, the formal scaling of the $^\phi$ ERI evaluation step is reduced from $\mathcal{O}(M^5)$ to $\mathcal{O}(M^2)$. It is not immediately obvious why Eq. (11) should hold true, especially in view of Eq. (10), but numerical data supports it.^{33–51} The NDDO approximation, Eq. (11), contains two central statements which are illustrated in Figure 1 at the example of water. First, the NDDO approximation states that a $^\phi$ ERI will be similar to a x ERI if χ_μ^I and χ_ν^J are centered on the same atom ($I = J$) and χ_λ^K and χ_σ^L are centered on the same atom ($K = L$), i.e., $\delta_{IJ} \delta_{KL} = 1$,

$$\langle \phi_\mu \phi_\nu | \phi_\lambda \phi_\sigma \rangle \approx \langle \chi_\mu^I \chi_\nu^I | \chi_\lambda^K \chi_\sigma^K \rangle. \quad (12)$$

We can see that this approximation is valid for the water example because the red circles in Figure 1 (left) are located close to the diagonal dashed line. Second, the NDDO approximation states that a $^\phi$ ERI will be zero if χ_μ^I and χ_ν^J are not centered on the same atom ($I \neq J$) or if χ_λ^K and χ_σ^L are not centered on the same atom ($K \neq L$), i.e., $\delta_{IJ} \delta_{KL} = 0$. Consequently, the blue crosses in Figure 1 have to lie close to the horizontal dashed lines ($\langle \phi_\mu \phi_\nu | \phi_\lambda \phi_\sigma \rangle = 0$) for the NDDO approximation to be reliable. If a blue cross does not lie close to this horizontal dashed line, it will indicate that the NDDO approximation does not hold. We examine the errors that Eq. (11) introduces in $^\phi$ ERIs in detail.

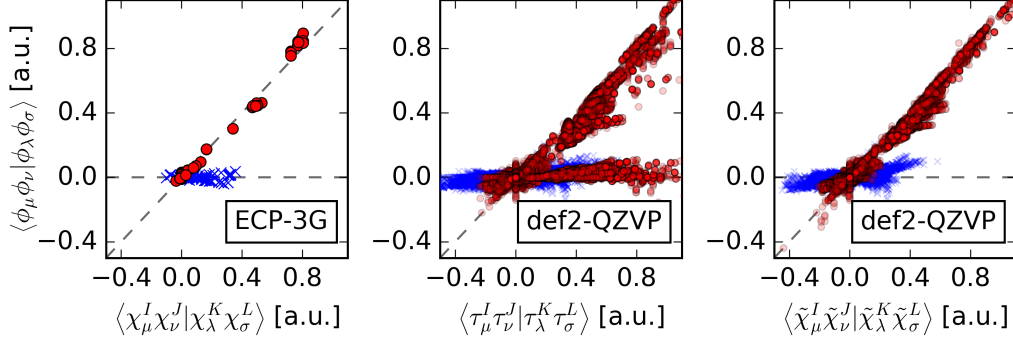


Figure 1: ϕ ERIs (y-axis), χ ERIs (x-axis, left), τ ERIs (x-axis, middle), and χ ERIs after local orthogonalization (x-axis, right) for the water molecule in an ECP-3G^{7,63} basis set (left) and in a def2-QZVP⁶⁴ basis set (middle and right). The NDDO approximation holds if the red circles ($I = J$ and $K = L$) lie on the diagonal gray dashed line and if the blue crosses ($I \neq J$ or $K \neq L$) lie on the horizontal dashed line.

Throughout this work, we denote the error which arises from the application of Eq. (11) instead of Eq. (10) by \mathcal{E} . The superscript to \mathcal{E} indicates which quantity is affected; additional specifications are then given as subscripts. For example, the error introduced by the NDDO approximation for the ϕ ERI $\langle \phi_\mu \phi_\nu | \phi_\lambda \phi_\sigma \rangle$ is denoted as $\mathcal{E}_{\mu\nu\lambda\sigma}^{\phi\text{ERI}}$. We define $\mathcal{E}_{\mu\nu\lambda\sigma}^{\phi\text{ERI}}$ as the deviation of $\delta_{IJ}\delta_{KL} \langle \chi_\mu^I \chi_\nu^J | \chi_\lambda^K \chi_\sigma^L \rangle$ from the analytical value of $\langle \phi_\mu \phi_\nu | \phi_\lambda \phi_\sigma \rangle$,

$$\mathcal{E}_{\mu\nu\lambda\sigma}^{\phi\text{ERI}} = \langle \phi_\mu \phi_\nu | \phi_\lambda \phi_\sigma \rangle - \delta_{IJ}\delta_{KL} \langle \chi_\mu^I \chi_\nu^J | \chi_\lambda^K \chi_\sigma^L \rangle. \quad (13)$$

Obviously, M^4 different errors $\mathcal{E}_{\mu\nu\lambda\sigma}^{\phi\text{ERI}}$ need to be accounted for.

We then consider the effect of erroneous ϕ ERIs on the HF energy when the self-consistent solution ${}^\phi\mathbf{C}$ obtained from an exact HF calculation is applied. The errors in the ϕ ERIs affect the Coulomb matrix elements,

$${}^\phi J_{\mu\nu}({}^\phi\mathbf{C}) \approx {}^\chi J_{\mu\nu}^{\text{NDDO}}({}^\phi\mathbf{C}) = \sum_{\lambda\sigma}^M {}^\phi P_{\lambda\sigma}({}^\phi\mathbf{C}) \delta_{IJ} \delta_{KL} \langle \chi_\mu^I \chi_\nu^J | \chi_\lambda^K \chi_\sigma^L \rangle, \quad (14)$$

and the exchange matrix elements,

$${}^\phi K_{\mu\nu}({}^\phi\mathbf{C}) \approx {}^\chi K_{\mu\nu}^{\text{NDDO}}({}^\phi\mathbf{C}) = -\frac{1}{2} \sum_{\lambda\sigma}^M {}^\phi P_{\lambda\sigma}({}^\phi\mathbf{C}) \delta_{IL} \delta_{JK} \langle \chi_\mu^I \chi_\sigma^L | \chi_\lambda^K \chi_\nu^J \rangle. \quad (15)$$

Interestingly, the matrix element $\phi J_{\mu\nu}$ will always be exactly zero if χ_μ^I and χ_ν^J are centered on different atoms ($I \neq J$) irrespective of the number of atoms on which χ_λ^K and χ_σ^L are centered (see Figure 2). By contrast, $\phi K_{\mu\nu}$ will not be strictly zero in this case (see also Figure 2). By affecting the

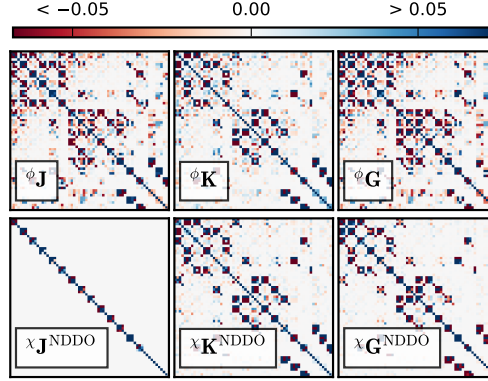


Figure 2: Graphical representation of $\phi \mathbf{J}(\phi \mathbf{C})$, $\phi \mathbf{K}(\phi \mathbf{C})$, and $\phi \mathbf{G}(\phi \mathbf{C})$ (left to right in upper panel) and of $\chi \mathbf{J}^{\text{NDDO}}(\phi \mathbf{C})$, $\chi \mathbf{K}^{\text{NDDO}}(\phi \mathbf{C})$, and $\chi \mathbf{G}^{\text{NDDO}}(\phi \mathbf{C})$ (left to right in lower panel) of the caffeine molecule (ECP-3G basis set). The matrices were evaluated with a density matrix determined from a fully converged HF calculation yielding $\phi \mathbf{C}$. They are colored according to their values ranging from -0.05 a.u. (red) to zero (white) to 0.05 a.u. (blue).

Coulomb and exchange matrices, the NDDO approximation will introduce an error compared to $E_{\text{el}}^{\text{HF}}$ which we denote by $\mathcal{E}^{\text{HF}} = \mathcal{E}_{\text{el}}^{\text{HF}}$,

$$\begin{aligned} \mathcal{E}^{\text{HF}} &= E_{\text{el}}^{\text{HF}}(\phi \mathbf{C}) - E_{\text{el}}^{\text{HF-NDDO}}(\phi \mathbf{C}), \\ &= \frac{1}{2} \sum_{\mu\nu\lambda\sigma}^M \phi P_{\nu\mu}(\phi \mathbf{C}) \phi P_{\lambda\sigma}(\phi \mathbf{C}) \left[\mathcal{E}_{\mu\nu\lambda\sigma}^{\phi \text{ERI}} - \frac{1}{2} \mathcal{E}_{\mu\sigma\lambda\nu}^{\phi \text{ERI}} \right], \end{aligned} \quad (16)$$

in the closed-shell case.

If we apply the NDDO approximation, we, however, must iterate to self consistency. The self-consistently obtained $\chi \mathbf{C}^{\text{NDDO}}$ will likely not be the same as $\phi \mathbf{C}$. Hence, another error arises from the NDDO approximation by introducing errors in other quantities during the self-consistent-field (SCF) cycles, i.e., in the coefficient matrix and in the matrix of orbital energies. We

denote this error by \mathcal{G} and again indicate by a superscript which quantity is affected by the error (and give additional specifications as subscripts). By contrast, \mathcal{E} denotes the error that is obtained when applying ${}^\phi\mathbf{C}$. The difference of the two self-consistent solutions produces $\mathcal{G}^{\text{HF}} = \mathcal{G}_{\text{el}}^{E^{\text{HF}}}$,

$$\begin{aligned} \mathcal{G}^{\text{HF}} &= E_{\text{el}}^{\text{HF}}({}^\phi\mathbf{C}) - E_{\text{el}}^{\text{HF-NDDO}}({}^x\mathbf{C}^{\text{NDDO}}), \\ &= \sum_{\mu\nu}^M ({}^\phi P_{\nu\mu}({}^\phi\mathbf{C}) - {}^x P_{\nu\mu}^{\text{NDDO}}({}^x\mathbf{C}^{\text{NDDO}})) \langle \phi_\mu | \hat{h} | \phi_\nu \rangle \\ &\quad + \frac{1}{2} \sum_{\mu\nu\lambda\sigma}^M \left({}^\phi P_{\nu\mu}({}^\phi\mathbf{C}) {}^\phi P_{\lambda\sigma}({}^\phi\mathbf{C}) \left[\langle \phi_\mu \phi_\nu | \phi_\lambda \phi_\sigma \rangle - \frac{1}{2} \langle \phi_\mu \phi_\sigma | \phi_\lambda \phi_\nu \rangle \right] \right. \\ &\quad \left. - {}^x P_{\nu\mu}^{\text{NDDO}}({}^x\mathbf{C}^{\text{NDDO}}) {}^x P_{\lambda\sigma}^{\text{NDDO}}({}^x\mathbf{C}^{\text{NDDO}}) \left[\delta_{IJ} \delta_{KL} \langle \chi_\mu^I \chi_\nu^J | \chi_\lambda^K \chi_\sigma^L \rangle \right. \right. \\ &\quad \left. \left. - \frac{1}{2} \delta_{IL} \delta_{JK} \langle \chi_\mu^I \chi_\sigma^L | \chi_\lambda^K \chi_\nu^J \rangle \right] \right). \end{aligned} \quad (17)$$

The electronic HF energy does, by definition, not contain effects from electron correlation.⁵⁵ Various electronic structure methods are available for calculating correlation energies.⁵⁵ The prevalent single- and multi-reference methods require the calculation of ERIs in the molecular orbital basis ψ (${}^\psi$ ERIs). These ${}^\psi$ ERIs are obtained through a 4-index transformation of the ${}^\phi$ ERIs (or the x ERIs),

$$\langle \psi_i \psi_j | \psi_k \psi_l \rangle = \sum_{\mu\nu\lambda\sigma}^M {}^\phi C_{\mu i} {}^\phi C_{\nu j} \langle \phi_\mu \phi_\nu | \phi_\lambda \phi_\sigma \rangle {}^\phi C_{\lambda k} {}^\phi C_{\sigma l}. \quad (18)$$

This 4-index transformation is similar to the 4-index transformation with which the ${}^\phi$ ERIs are determined from the x ERIs (Eq. (10)). When applying Eq. (11), we may approximate the ${}^\psi$ ERIs as,

$$\langle \psi_i \psi_j | \psi_k \psi_l \rangle \approx \sum_{\mu\nu\lambda\sigma}^M {}^\phi C_{\mu i} {}^\phi C_{\nu j} \delta_{IJ} \delta_{KL} \langle \chi_\mu^I \chi_\nu^J | \chi_\lambda^K \chi_\sigma^L \rangle {}^\phi C_{\lambda k} {}^\phi C_{\sigma l}. \quad (19)$$

The formal scaling of the ${}^\psi$ ERI evaluation step is therefore reduced from $\mathcal{O}(M^5)$ to $\mathcal{O}(M^2)$ scaling which comes at the price of an error in the M^4 ${}^\psi$ ERIs, $\mathcal{E}_{ijkl}^{\psi\text{ERI}}$,

$$\mathcal{E}_{ijkl}^{\psi\text{ERI}} = \sum_{\mu\nu\lambda\sigma}^M {}^\phi C_{\mu i} {}^\phi C_{\nu j} \mathcal{E}_{\mu\nu\lambda\sigma}^{\phi\text{ERI}} {}^\phi C_{\lambda k} {}^\phi C_{\sigma l}. \quad (20)$$

If we determine the coefficient matrix in a self-consistent field procedure, we will introduce an additional error $\mathcal{G}_{ijkl}^{\psi\text{ERI}}$ from applying a different coefficient matrix,

$$\mathcal{G}_{ijkl}^{\psi\text{ERI}} = \sum_{\mu\nu\lambda\sigma}^M \left({}^\phi C_{\mu i} {}^\phi C_{\nu j} \langle \phi_\mu \phi_\nu | \phi_\lambda \phi_\sigma \rangle {}^\phi C_{\lambda k} {}^\phi C_{\sigma l} - {}^\chi C_{\mu i}^{\text{NDDO}\chi} {}^\chi C_{\nu j}^{\text{NDDO}} \delta_{IJ} \delta_{KL} \langle \chi_\mu^I \chi_\nu^J | \chi_\lambda^K \chi_\sigma^L \rangle {}^\chi C_{\lambda k}^{\text{NDDO}\chi} {}^\chi C_{\sigma l}^{\text{NDDO}} \right). \quad (21)$$

In this work, we demonstrate how $\mathcal{E}_{ijkl}^{\psi\text{ERI}}$ and $\mathcal{G}_{ijkl}^{\psi\text{ERI}}$ affect the MP2 correlation energies. We denote the total MP2 energies as $E_{\text{el}}^{\text{MP2}}$ which is then given as

$$E_{\text{el}}^{\text{MP2}} = E_{\text{el}}^{(0)} + E_{\text{el}}^{(1)} + E_{\text{el}}^{(2)} = E_{\text{el}}^{\text{HF}} + E_{\text{el}}^{(2)}, \quad (22)$$

where $E_{\text{el}}^{(0)}$, $E_{\text{el}}^{(1)}$, and $E_{\text{el}}^{(2)}$ denote the low-order perturbation-theory contributions. We quantify $\mathcal{E}^{(2)} = \mathcal{E}^{E_{\text{el}}^{(2)}}$ and $\mathcal{G}^{(2)} = \mathcal{G}^{E_{\text{el}}^{(2)}}$, respectively, by subtracting $E_{\text{el}}^{(2)}$ obtained when invoking the NDDO approximation from the exact $E_{\text{el}}^{(2)}$.

2.3 Extension to Conventional Basis Sets

By definition, the χ -basis fulfills the condition that it is locally orthogonal. Ordinary basis sets are, in general, not locally orthogonal which we illustrate in Figure 3 for the example of water and a def2-QZVP basis set. If the basis set would be locally orthogonal, we would not have any off-diagonal entries in the green boxes in Figure 3. We denote such ordinary Gaussian-type basis functions by τ_μ^I (μ -th basis function of type τ centered on atom I). The NDDO approximation is not straightforwardly applicable for an arbitrary τ -basis which is also illustrated in Figure 1 (middle). When we apply an ordinary basis set, such as the def2-QZVP basis set,⁶⁴ many of the red circles are not located close to the diagonal dashed lines anymore, i.e.,

$$\langle \phi_\mu \phi_\nu | \phi_\lambda \phi_\sigma \rangle \not\approx \langle \tau_\mu^I \tau_\nu^I | \tau_\lambda^K \tau_\sigma^K \rangle. \quad (23)$$

To cure this problem, we propose to transform $\{\tau_\mu^I\}$ to a locally orthogonal basis $\{\chi_\mu^I\}$ by the application of the transformation matrix \mathbf{T} (see Figure 3),

$$T_{\mu\nu} = \delta_{IJ} ({}^\chi S^{-\frac{1}{2}})_{\mu\nu}, \quad (24)$$

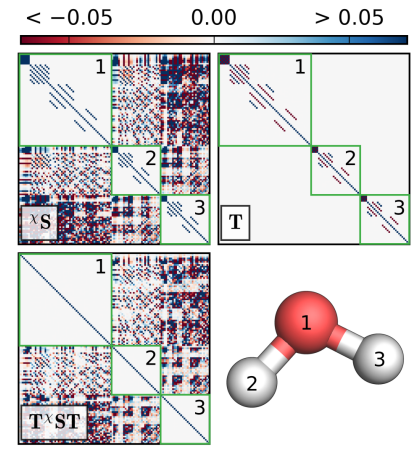


Figure 3: Graphical representation of ${}^{\chi}\mathbf{S}$, \mathbf{T} , and $\mathbf{T}^{\chi}\mathbf{ST}$ for a water molecule (def2-QZVP basis set). The entries according to their values ranging from -0.05 (red) to zero (white) to 0.05 (blue). The blocks for which the respective basis functions are centered on the same atom are highlighted in green.

so that

$$\tilde{\chi}_{\nu}^J = \sum_{\mu=1}^M T_{\mu\nu} \tau_{\mu}^I, \quad (25)$$

where the tilde indicates that the local orthogonal basis function $\tilde{\chi}$ was obtained by means of a transformation of a τ -basis. Figure 3 illustrates that the basis $\tilde{\chi}$ for the water example is locally orthogonal which is evident from the fact that there are no nonzero off-diagonal elements in the green boxes for $\mathbf{T}^{\chi}\mathbf{ST}$. Figure 1 (right) shows that all red circles are located close to the diagonal dashed line after local orthogonalization, i.e., the validity of the NDDO approximation has been restored.

3 Analysis of the NDDO Approximation for Molecules in a χ -Basis

For the first part of our analysis of the NDDO approximation, we applied the ECP-3G basis set.^{7,63} We selected the ECP-3G basis set because its basis

functions form a χ -basis and because it is applied (in slightly modified forms) in the OM1, OM2, and OM3 models.^{7–9} The ECP-3G basis set specifies one s -type basis function for hydrogen and one s -type and three p -type basis functions for carbon, nitrogen, oxygen, and fluorine. We consider four different sets of molecular structures for this part of the analysis: (A) We first analyze the NDDO approximation on the simplest possible model system which is a dihydrogen molecule $\text{H}_1\text{—H}_2$ with an interatomic distance R_{12} . This is the simplest possible model system because NDDO is no approximation for isolated atoms (where $\phi = \chi$) and for systems with only one electron (e.g., H_2^+). (B) We assemble a series of linear alkane chains $\text{C}_x\text{H}_{2x+2}$, $x = 1, 2, \dots, 15$ to study trends with an increasing molecular size. (C) We randomly select a subset of 5000 molecules of the QM9 data set^{65,66} which allows us to examine the NDDO approximation for a variety of equilibrium structures of molecules composed of H, C, N, O, and F. (D) We choose three reaction trajectories, a Diels–Alder reaction between butadiene and ethylene yielding cyclohexene (reaction A), the decomposition of azobisisobutyronitrile (reaction E), and the elimination of CO_2 from the benzoyl radical (reaction F) which we published in previous work.³¹

3.1 Effect on Electron-Electron Repulsion Integrals

For the simplest possible model system, H_2 , $2^4 = 16$ ERIs arise for a given R_{12} . Due to symmetry relations, only four of these 16 values are different,⁵⁴ so that it suffices to discuss $\mathcal{E}_{1111}^{\phi\text{ERI}}$, $\mathcal{E}_{1122}^{\phi\text{ERI}}$, $\mathcal{E}_{1212}^{\phi\text{ERI}}$, and $\mathcal{E}_{1112}^{\phi\text{ERI}}$ (see Figure 4). If the NDDO approximation would be valid, $\langle \chi_1^{\text{H}_1} \chi_1^{\text{H}_1} | \chi_1^{\text{H}_1} \chi_1^{\text{H}_1} \rangle$ would be similar to $\langle \phi_1 \phi_1 | \phi_1 \phi_1 \rangle$ (red lines in left and middle panels of Figure 4, respectively) and $\langle \chi_1^{\text{H}_1} \chi_1^{\text{H}_1} | \chi_2^{\text{H}_2} \chi_2^{\text{H}_2} \rangle$ would be similar to $\langle \phi_1 \phi_1 | \phi_2 \phi_2 \rangle$ (blue lines in left and middle panels of Figure 4, respectively). The right panel of Figure 4 visualizes the resulting error in these two ϕ ERIs. The error introduced by the NDDO approximation in $\langle \phi_1 \phi_1 | \phi_1 \phi_1 \rangle$ and $\langle \phi_1 \phi_1 | \phi_2 \phi_2 \rangle$ is large (> 0.02 a.u.) for $R_{12} < 2.0$ Å. Only if the overlap between $\chi_1^{\text{H}_1}$ and $\chi_2^{\text{H}_2}$ is small at large R_{12} , i.e., where the χ -basis becomes a ϕ -basis, $|\mathcal{E}_{1111}^{\phi\text{ERI}}|$ and $|\mathcal{E}_{1122}^{\phi\text{ERI}}|$ will be small. The ϕ ERIs $\langle \phi_1 \phi_2 | \phi_1 \phi_2 \rangle$ and $\langle \phi_1 \phi_1 | \phi_1 \phi_2 \rangle$ are assumed to be zero in the NDDO

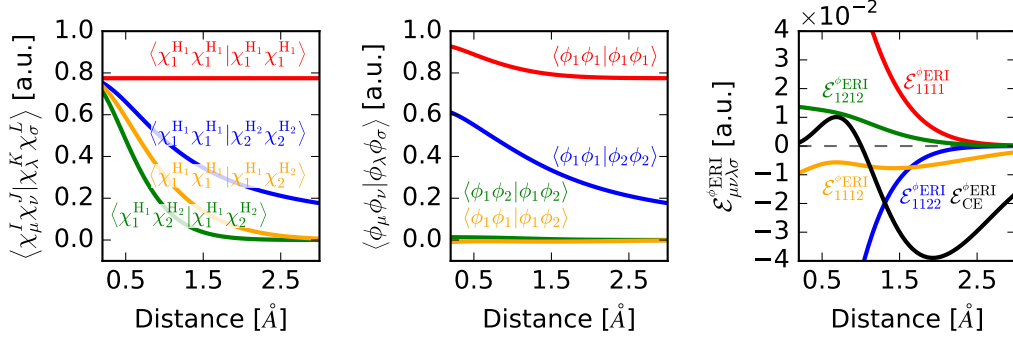


Figure 4: Dependence of the x ERIs (left), the ϕ ERIs (middle), and the error in the ϕ ERIs (right) on R_{12} in an H_2 molecule described by an ECP-3G basis. If the NDDO approximation would hold true, the error in the ϕ ERIs would be zero for every distance.

approximation (green and orange lines in the middle panel of Figure 4) which seems to be a good approximation. Figure 4 clearly illustrates that the corresponding x ERIs are not zero. For $R_{12} < 1.6$ Å, $|\mathcal{E}_{1212}^{\phi\text{ERI}}|$ and $|\mathcal{E}_{1112}^{\phi\text{ERI}}|$ are smaller than $|\mathcal{E}_{1111}^{\phi\text{ERI}}|$ and $|\mathcal{E}_{1122}^{\phi\text{ERI}}|$. For R_{12} larger than 1.6 Å, $\mathcal{E}_{1112}^{\phi\text{ERI}}$ is the largest individual error in a ϕ ERI. This gives rise to a large cumulative error (CE) $\mathcal{E}_{\text{CE}}^{\phi\text{ERI}}$,

$$\mathcal{E}_{\text{CE}}^{\phi\text{ERI}} = \sum_{\mu\nu\lambda\sigma}^M \mathcal{E}_{\mu\nu\lambda\sigma}^{\phi\text{ERI}}, \quad (26)$$

for $1.6 \text{ Å} < R_{12} < 3.0 \text{ Å}$. For $1.6 \text{ Å} < R_{12} < 3.0 \text{ Å}$, we find a significant error in at least one of the ϕ ERIs.

We also encounter nonnegligible $\mathcal{E}_{\mu\nu\lambda\sigma}^{\phi\text{ERI}}$ for all structures in the sets of molecules B, C, and D. The largest absolute error of a ϕ ERI in a given molecule is between 0.10 a.u. and 0.23 a.u. It is already obvious at this point that only an efficient error cancellation may yield useful observables based on these erroneous ϕ ERIs (and on density matrices obtained with them in SCF procedures).

Figure 5 shows that the cumulative absolute error (CAE) in the ϕ ERIs,

$$\mathcal{E}_{\text{CAE}}^{\phi\text{ERI}} = \sum_{\mu\nu\lambda\sigma}^M |\mathcal{E}_{\mu\nu\lambda\sigma}^{\phi\text{ERI}}|, \quad (27)$$

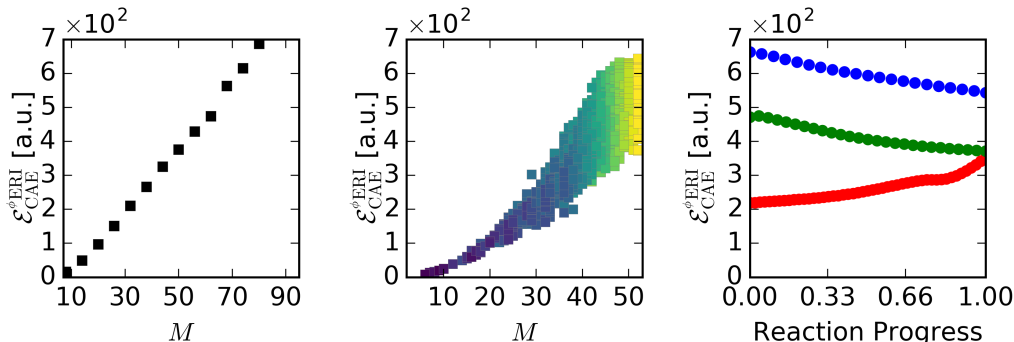


Figure 5: Dependence of the cumulative absolute error $\mathcal{E}_{\text{CAE}}^{\phi_{\text{ERI}}}$ (Eq. (27)) on the number of basis functions M for the molecule sets B (left), C (middle), and D (right). The entries for molecule set C are colored according to the number of atoms from purple (3 atoms) over blue (12 atoms) to yellow (25 atoms) and the ones for molecule set C according to the reaction: Reaction A (34 basis functions; red circles), reaction E (60 basis functions; blue circles), and reaction F (41 basis functions; green circles). All calculations were carried out with the ECP-3G basis.

grows roughly linearly with the number of basis functions for molecule set B (Figure 5). We observe a linear growth not only in the overall cumulative absolute error, but also in individual contributions to it when we break down the corresponding χ ERIs in one-, two-, three-, and four-center χ ERIs (see Figure S1 in the Supporting Information). Figure 5 shows that $\mathcal{E}_{\text{CAE}}^{\phi_{\text{ERI}}}$ also grows approximately linearly with the number of basis functions for C and that the spread of the individual $\mathcal{E}_{\text{CAE}}^{\phi_{\text{ERI}}}$ is large. In agreement with previous studies,^{42,46–50} we find that the assumption that the ϕ ERIs corresponding to $\langle \chi_{\mu}^I \chi_{\nu}^I | \chi_{\lambda}^J \chi_{\sigma}^K \rangle$ for $I \neq J \neq K$ and $\langle \chi_{\mu}^I \chi_{\nu}^I | \chi_{\lambda}^I \chi_{\sigma}^J \rangle$ for $I \neq J$ are zero is responsible for 60–65% of the overall cumulative absolute error for the molecule sets B and C (see Figure S1 in the Supporting Information). Furthermore, the change of $\mathcal{E}_{\text{CAE}}^{\phi_{\text{ERI}}}$ with reaction progress for D in Figure 5 shows that the cumulative absolute error in the ϕ ERIs crucially depends on the arrangement of the atomic nuclei, i.e. on the underlying nuclear framework that generates the external potential. If the cumulative absolute error in the ϕ ERIs would

not depend on the arrangement of the atomic nuclei, it would not change in the course of the reaction.

3.2 Error Propagation: the Hartree–Fock Energy

For H_2 , \mathcal{E}^{HF} depends linearly on the cumulative error of the ϕERIs because $\phi\mathbf{C}$ can be determined analytically,⁵⁴

$$\mathcal{E}^{\text{HF}} = \frac{1}{4}\mathcal{E}_{\text{CE}}^{\phi\text{ERI}} = \frac{1}{2}\mathcal{E}_{1111}^{\phi\text{ERI}} + \frac{1}{2}\mathcal{E}_{1122}^{\phi\text{ERI}} + \mathcal{E}_{1212}^{\phi\text{ERI}} + 2\mathcal{E}_{1112}^{\phi\text{ERI}}. \quad (28)$$

Previous results show that the NDDO approximation introduces an error of 0.002 a.u. for H_2 with $R_{12} = 0.84 \text{ \AA}$ ^{51,67} which we can reproduce. In our detailed analysis however, we also see that this value of R_{12} falls into the region where $\mathcal{E}_{\text{CE}}^{\phi\text{ERI}}$ is small due to a fortunate error cancellation of $\frac{1}{2}\mathcal{E}_{1111}^{\phi\text{ERI}}$, $\frac{1}{2}\mathcal{E}_{1122}^{\phi\text{ERI}}$, $\mathcal{E}_{1212}^{\phi\text{ERI}}$, and $2\mathcal{E}_{1112}^{\phi\text{ERI}}$ (see right panel of Figure 4). For larger or smaller R_{12} , we encounter larger \mathcal{E}^{HF} because the errors in the ϕERIs do not cancel as effectively.

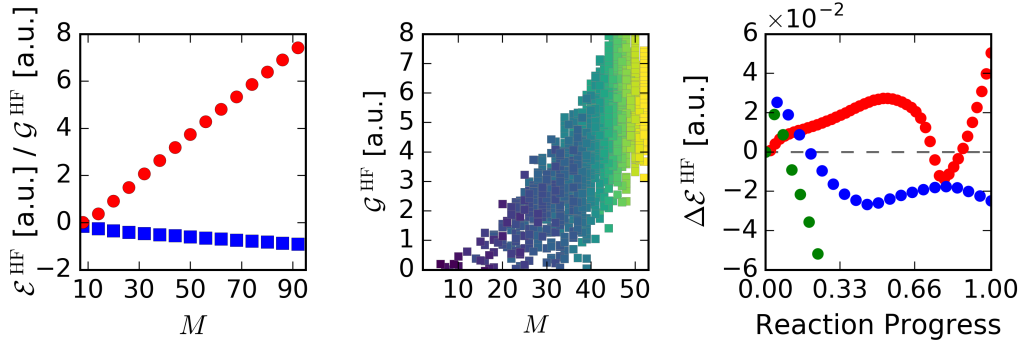


Figure 6: Left: Dependence of \mathcal{E}^{HF} (blue squares) and \mathcal{G}^{HF} (red circles) on the number of basis functions M for molecules in B. Middle: Dependence of \mathcal{G}^{HF} on M for molecules in C. The entries for molecule set C are colored according to the number of atoms from purple (3 atoms) over blue (12 atoms) to yellow (25 atoms). Right: Change in \mathcal{E}^{HF} with the reaction progress for reaction A (red circles), reaction E (blue circles), and reaction F (green circles). All calculations were carried out with an ECP-3G basis set.

For the calculation of E^{HF} , the ϕ ERIs are contracted with elements of the density matrix. The elements of the density matrix are therefore a central ingredient for an efficient error cancellation. We see how differently the errors in the ϕ ERIs add up by comparing \mathcal{E}^{HF} and \mathcal{G}^{HF} for the molecule set B in Figure 6. Interestingly, $|\mathcal{E}^{\text{HF}}|$ and \mathcal{G}^{HF} increase in an almost perfectly linear fashion with the number of basis functions. For a given number of basis functions, \mathcal{G}^{HF} is significantly larger than $|\mathcal{E}^{\text{HF}}|$ for molecule set B. We also see a roughly linear increase of \mathcal{G}^{HF} with the number of basis functions for the diverse organic molecules contained in set C. The errors in the HF energies also depend crucially on the arrangement of the atomic nuclei which we demonstrate in the right panel of Figure 6. In line with previous studies,^{35,42,46–51} we see that the NDDO approximation is a rather crude approximation. We discuss strategies to overcome this situation in Section 5.

3.3 Error Propagation: the MP2 Energy

The error in the ϕ ERIs also propagates to the ψ ERIs (Eq. (19)). We show the effect of the NDDO approximation on selected ψ ERIs, $\langle\psi_1\psi_1|\psi_1\psi_1\rangle$, $\langle\psi_1\psi_1|\psi_2\psi_2\rangle$, $\langle\psi_2\psi_2|\psi_2\psi_2\rangle$, and $\langle\psi_1\psi_2|\psi_1\psi_2\rangle$, in H_2 in Figure 7. We choose

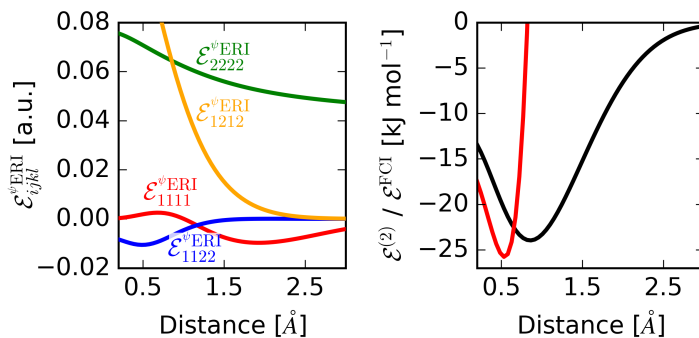


Figure 7: Dependence of the error in selected ψ ERIs (left), \mathcal{E}^{MP2} (black line; right), and \mathcal{E}^{FCI} (red line; right) on R_{12} in the H_2 molecule described in an ECP-3G basis.

to study these ψ ERIs because they are applied in the calculation of the $E_{\text{el}}^{(2)}$

($\langle\psi_1\psi_1|\psi_2\psi_2\rangle$) and of the full-configuration interaction (FCI) correlation energy⁵⁴ (all of these ψ ERIs). All of these ψ ERIs are significantly affected by the NDDO approximation. Hence, it comes as no surprise that the MP2 and FCI correlation energies are deteriorated by the NDDO approximation. The general shape of $E_{\text{el}}^{(2)}$ follows that of $\mathcal{E}_{1122}^{\psi\text{ERI}}$ and has a minimum at $R_{12} = 0.86$ Å where $\mathcal{E}^{(2)} = -0.009$ a.u. As a consequence, instead of $E_{\text{el}}^{(2)} = -0.016$ a.u. a $E_{\text{el}}^{(2)} = -0.007$ a.u. is obtained when the NDDO approximation is invoked. The MP2 correlation energy is therefore significantly underestimated. The FCI correlation energy is also significantly underestimated for $R_{12} < 0.72$ Å. An unfortunate addition of the errors in $\langle\psi_2\psi_2|\psi_2\psi_2\rangle$ and $\langle\psi_1\psi_1|\psi_1\psi_1\rangle$, however, leads to an overestimation of E^{FCI} for $R_{12} \geq 0.72$ Å. The errors in the ψ ERIs and, hence, in E^{FCI} , only vanish in the limit of very large R_{12} ($R_{12} > 25.0$ Å).

The NDDO approximation also deteriorates the MP2 energies for the other molecules that we investigated (see Figure 8). Interestingly, the NDDO approximation always produced too small MP2 correlation energies. The amount by which $E_{\text{el}}^{(2)}$ is underestimated depends roughly linearly on the number of basis functions so that $E_{\text{el}}^{(2)}$ is underestimated by -0.15 a.u. for a molecule with 25 basis functions and by -0.30 a.u. for a molecule with 50 basis functions. The significance of these results becomes apparent in the context of previous studies which reported far too small correlation energies determined for NDDO-SEMO reference wave functions.^{68,69} Our results can be taken as an indication that the low correlation energies arise as a direct consequence of the NDDO approximation and not of the introduction of other parametrized expressions when assembling NDDO-SEMO models.

4 Analysis of the NDDO Approximation for Molecules in the τ -Basis

When applying ordinary τ -basis sets, large errors in the ϕ ERIs arise. For H_2 and $R_{12} = 0.74$ Å described in a cc-pVDZ basis set,⁷⁰ for example, the largest absolute error in a ϕ ERI amounts to 0.51 a.u. The application of these erro-

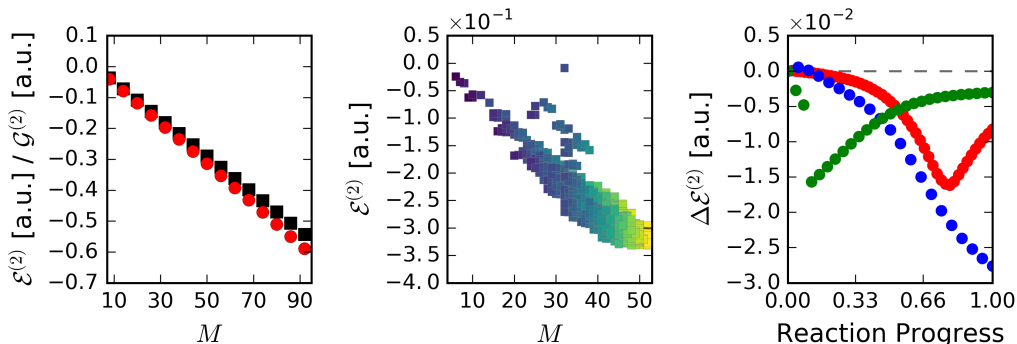


Figure 8: Left: Dependence of $\mathcal{E}^{(2)}$ (black squares) and \mathcal{G}^{MP2} (red circles) on the number of basis functions for molecules in set B. Middle: Dependence of $\mathcal{E}^{(2)}$ on the number of basis functions for molecules in set C. The entries for molecule set C are colored according to the number of atoms from purple (3 atoms) over blue (12 atoms) to yellow (25 atoms). Right: Dependence of $\mathcal{E}^{(2)}$ on the reaction progress for reaction A (red circles), reaction E (blue circles), and reaction F (green circles). All calculations were carried out with the ECP-3G basis set.

neous ϕ ERIs even leads to a $E_{\text{el}}^{\text{HF}} = -0.55$ a.u. which is far too large compared to the exact $E_{\text{el}}^{\text{HF}} = -1.13$ a.u. After the local orthogonalization (Eq. (25)) of the basis set, we obtain $\mathcal{G}^{\text{HF}} = 0.01$ a.u. A prior local orthogonalization led to significantly smaller largest absolute errors in the ϕ ERIs and cumulative errors in the ϕ ERIs for all molecules (B, C, and D) by up to an order of magnitude (see also Table S3 in the Supporting Information).

We found a fundamental limitation of the NDDO approximation in the course of our analysis of different τ -basis sets, i.e., cc-pVXZ ($X = \text{D},^{70} \text{T},^{70} \text{Q},^{70} 5,^{70} 6,^{71}$ see Figure 9): Usually, $E_{\text{el}}^{\text{HF}}$ converges smoothly to the HF limit when larger and larger basis sets are applied. The HF limit for H_2 for $R_{12} = 0.74$ Å was determined to be $E_{\text{el}}^{\text{HF}} = -1.133629$ a.u.⁷² When applying a cc-pV6Z basis set, we obtain $E_{\text{el}}^{\text{HF}} = -1.133476$. Figure 9 shows that the HF energies calculated with the NDDO approximation do not converge with respect to the basis-set size. Furthermore, we obtained $E_{\text{el}}^{\text{HF}}$ that are smaller than the HF limit which is worrisome.

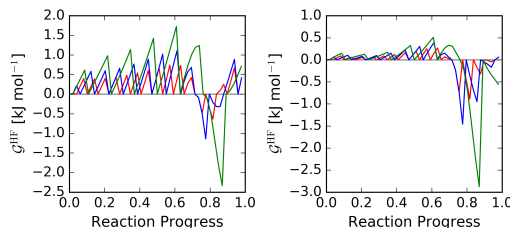


Figure 9: $E_{\text{el}}^{\text{HF}}$ for H_2 for $R_{12} = 0.74 \text{ \AA}$ in a.u. calculated without (black lines) and with (red and blue lines) the NDDO approximation and different basis sets. We calculated $E_{\text{el}}^{\text{HF}}$ with the NDDO approximation either self-consistently (red lines) or non-self-consistently, i.e., with orbitals taken from the HF reference calculation (blue lines). For reference, we provide the HF-limit energy $E_{\text{el}}^{\text{HF}} = -1.133629 \text{ a.u.}$ ⁷²

5 Improving on the NDDO Approximation

The NDDO approximation introduces significant errors in the ϕ ERIs, observed here for the simplest possible neutral molecule, H_2 , and for a diverse selection of medium-sized organic compounds. Obviously, these errors are too large and too unsystematic for the NDDO approximation to be useful in purely *ab initio* electronic structure models.

5.1 Modifications

In *ab initio* electronic structure calculations, it is customary to apply screening techniques to determine which χ ERIs are negligibly small.⁵⁵ Errors are controlled by thresholds with respect to which the χ ERIs are neglected.⁵⁵ By contrast, the NDDO approximation cannot be applied as a screening tool for χ ERIs because it can only predict whether the corresponding ERIs in the ϕ -basis are negligibly small or not. Each ϕ ERI, however, encodes information on *all* χ ERIs (Eq. (10)). It is therefore computationally difficult to improve on the NDDO approximation by an explicit transformation of the ERIs from the χ - to the ϕ -basis because this is a 4-index transformation that scales as $\mathcal{O}(M^5)$. Some attempts^{51,73} were made to improve on the approximation of the ϕ ERIs for which the corresponding χ ERIs are one-

center ERIs ($\langle \chi_\mu^I \chi_\nu^I | \chi_\lambda^I \chi_\sigma^I \rangle$) and two-center ERIs ($\langle \chi_\mu^I \chi_\nu^I | \chi_\lambda^J \chi_\sigma^J \rangle$ for $I \neq J$). However, these suggestions did not find widespread use. Moreover, our results suggest that a correction of these ϕ ERIs does not suffice to obtain a reliable HF energy $E_{\text{el}}^{\text{HF}}$. A large portion of the error originates from the ϕ ERIs that are assumed to be zero, but are not exactly zero. For molecule set C, for example, these neglected ϕ ERIs on average make up 99% of the ϕ ERIs and these are responsible for 81% of the cumulative absolute error. If we had to estimate these ϕ ERIs, we would again need close to $\mathcal{O}(M^4)$ operations. These estimates would have to be accurate due to the plethora of small ϕ ERIs that would again compromise the computational efficiency of the NDDO approximation.

5.2 Capitalizing on Error Cancellation

In all popular NDDO-SEMO models, the one-center χ ERIs $\langle \chi_\mu^I \chi_\nu^I | \chi_\lambda^I \chi_\sigma^I \rangle$ are substituted for empirical parameters. These parameters are usually chosen to be smaller than the corresponding analytical one-center χ ERI.² The two-center χ ERIs $\langle \chi_\mu^I \chi_\nu^I | \chi_\lambda^J \chi_\sigma^J \rangle$ for $I \neq J$ are scaled so that they are also smaller than the corresponding analytical χ ERIs^{2,74} (see also Figure S2 in the Supporting Information). In MNDO-type models, the two-center χ ERIs are evaluated from a classical multipole expression truncated after the quadrupole contribution which was shown to have a negligible effect on the values of the two-center χ ERIs.⁷⁴ Because of the application of parametrized expressions to evaluate the one- and two-center χ ERIs, the results obtained with *ab initio* electronic structure methods invoking the NDDO approximation cannot be directly compared to results obtained with modern NDDO-SEMO models.

Furthermore, all successful NDDO-SEMO models introduce various parametric expressions to assemble the one-electron matrix and to calculate the nucleus-nucleus repulsion energy.^{2,4-9} For contemporary NDDO-SEMO models, the parametric expressions were designed such that the result of the SCF optimization yields a result close to a reference energy *despite* significant errors in the ϕ ERIs compared to the analytical analogues. Overall, the results obtained with NDDO-SEMO models achieve a remarkably high

accuracy with respect to these reference data.^{75,76} At the same time, NDDO-SEMO models are notoriously unreliable for molecules not considered in the parametrization procedure.^{75,76} It is virtually impossible to rationalize why errors occur due to the number and the diversity of the approximations invoked in an NDDO-SEMO model. At least some of these errors are likely to be due to the NDDO approximation.

The parameters in popular NDDO-SEMO models were determined in such a way that the SCF results deviate in a least-squares manner from experimental reference data. In line with the results reported in Section 3.3, the MP2 correlation energy $E_{\text{el}}^{(2)}$ obtained with respect to a HF-type reference wave function obtained with existing NDDO-SEMO models will generally be too small.^{68,69} The χ ERI scaling applied in NDDO-SEMO models (which makes the χ ERIs artificially smaller (see also Figure S2 in the Supporting Information)) will worsen the situation because the already too small ψ ERIs will become even smaller. Nevertheless, it might be possible to define a NDDO-SEMO model where the error in $E_{\text{el}}^{(0)} + E_{\text{el}}^{(1)}$ compensates for errors in a subsequent separately calculated $E_{\text{el}}^{\text{MP2}}$ in order to justify scaled ERIs (see also Eq. (22)). A first step in the direction of designing a SEMO model capable of reaching a satisfactory agreement with coupled cluster electronic energies was presented by Margraf *et al.*⁷⁷ This model is, however, restricted to single atoms and additional effort would be necessary to design a general-purpose NDDO-SEMO model. The focus of this work, however, is the effect of the NDDO approximation on the ERIs and we therefore directly compared ERIs with and without NDDO.

In general, we may anticipate that the improvement of the parametric expressions in the NDDO-SEMO models is as complicated as the direct correction for the error introduced by the NDDO approximation as discussed in Section 5.1. Therefore, the only viable use of NDDO-SEMO models appears to be their combination with system-focused rigorous error estimation schemes as proposed in Refs. 78,79.

5.3 Correcting the Two-Electron Matrices

We propose an alternative correction strategy, the correction inheritance to semiempirics (CISE) approach, which allows for rapid calculations invoking the NDDO approximation with error control. In 1969, Roby and Sinanoğlu made an attempt to accelerate single-point HF calculations for a diverse set of small molecules.³⁴ They suggested to scale ${}^{\chi}\mathbf{G}^{\text{NDDO}}$ with a matrix $\mathbf{\Gamma}$ to obtain a better estimate for ${}^{\phi}\mathbf{G}$,

$${}^{\phi}\mathbf{G} \approx \mathbf{\Gamma} {}^{\chi}\mathbf{G}^{\text{NDDO}}. \quad (29)$$

Their attempt to define general rules to assemble $\mathbf{\Gamma}$ turned out to be impossible.³⁴

In this Section, we reconsider and build upon the Roby–Sinanoğlu approach. We can exactly determine $\mathbf{\Gamma}(\{\tilde{\mathbf{R}}_I^n\})$ for a given structure $\{\tilde{\mathbf{R}}_I^n\}$ from a reference HF, KS-DFT, or multi-configurational SCF calculation (yielding the exact ${}^{\phi}\mathbf{G}^{\{\tilde{\mathbf{R}}_I^n\}}(\phi\mathbf{C})$),

$$\mathbf{\Gamma}^{\{\tilde{\mathbf{R}}_I^n\}}(\phi\mathbf{C}) = {}^{\phi}\mathbf{G}^{\{\tilde{\mathbf{R}}_I^n\}}(\phi\mathbf{C}) \cdot \left({}^{\chi}\mathbf{G}^{\text{NDDO}\{\tilde{\mathbf{R}}_I^n\}}(\phi\mathbf{C}) \right)^{-1}. \quad (30)$$

Figure 10 now shows that $\mathbf{\Gamma}^{\{\tilde{\mathbf{R}}_I^n\}}(\phi\mathbf{C})$ is transferable to a certain degree in a sequence of related structures. That is, for two similar structures $\{\tilde{\mathbf{R}}_I^n\}$ and $\{\tilde{\mathbf{R}}_I^{(n+1)}\}$ we have

$${}^{\phi}\mathbf{G}^{\{\tilde{\mathbf{R}}_I^{(n+1)}\}}(\phi\mathbf{C}) \approx \mathbf{\Gamma}^{\{\tilde{\mathbf{R}}_I^n\}}(\phi\mathbf{C}) \cdot {}^{\chi}\mathbf{G}^{\text{NDDO}\{\tilde{\mathbf{R}}_I^{(n+1)}\}}({}^{\chi}\mathbf{C}^{\text{NDDO}}). \quad (31)$$

Eq. (31) defines a system-focused NDDO model, the CISEmul model (‘mul’ for multiplicative), that can be applied in connection with any Fock operator.

The original Roby–Sinanoğlu approach is not the only one conceivable for the construction of correction matrices. In fact, a multiplicative correction matrix changes matrix elements through a combination of elements of the original matrix. An additive correction appears easier and more straightforward to achieve the goal of readjusting individual matrix elements. We may therefore define separate additive corrections with the matrices $\mathbf{\Gamma}_J$ and $\mathbf{\Gamma}_K$

to $\chi \mathbf{J}^{\text{NDDO}}$ and to $\chi \mathbf{K}^{\text{NDDO}}$,

$$\begin{aligned} \phi_{\mathbf{G}}\{\tilde{\mathbf{R}}_I^{(n+1)}\}(\phi \mathbf{C}) &\approx \Gamma_{\mathbf{J}}\{\tilde{\mathbf{R}}_I^n\}(\phi \mathbf{C}) + \chi \mathbf{J}^{\text{NDDO}}\{\tilde{\mathbf{R}}_I^{(n+1)}\}(\chi \mathbf{C}^{\text{NDDO}}) \\ &\quad + \Gamma_{\mathbf{K}}\{\tilde{\mathbf{R}}_I^n\}(\phi \mathbf{C}) + \chi \mathbf{K}^{\text{NDDO}}\{\tilde{\mathbf{R}}_I^{(n+1)}\}(\chi \mathbf{C}^{\text{NDDO}}), \end{aligned} \quad (32)$$

or a unification of $\Gamma_{\mathbf{J}}$ and $\Gamma_{\mathbf{K}}$ as a total additive correction (CISEadd approach where ‘add’ stands for additive). The correction matrices $\Gamma_{\mathbf{J}}$ and $\Gamma_{\mathbf{K}}$ may again be obtained from a reference HF, KS-DFT, or multi-configurational SCF calculation so that

$$\Gamma_{\mathbf{J}}\{\tilde{\mathbf{R}}_I^n\}(\phi \mathbf{C}) = \phi_{\mathbf{J}}\{\tilde{\mathbf{R}}_I^n\}(\phi \mathbf{C}) - \chi \mathbf{J}^{\text{NDDO}}\{\tilde{\mathbf{R}}_I^n\}(\phi \mathbf{C}) \quad (33)$$

and

$$\Gamma_{\mathbf{K}}\{\tilde{\mathbf{R}}_I^n\}(\phi \mathbf{C}) = \phi_{\mathbf{K}}\{\tilde{\mathbf{R}}_I^n\}(\phi \mathbf{C}) - \chi \mathbf{K}^{\text{NDDO}}\{\tilde{\mathbf{R}}_I^n\}(\phi \mathbf{C}). \quad (34)$$

We demonstrate the capabilities of the CISEmul and the CISEadd approach on the example of reaction A in Figure 10. If we do not correct for the

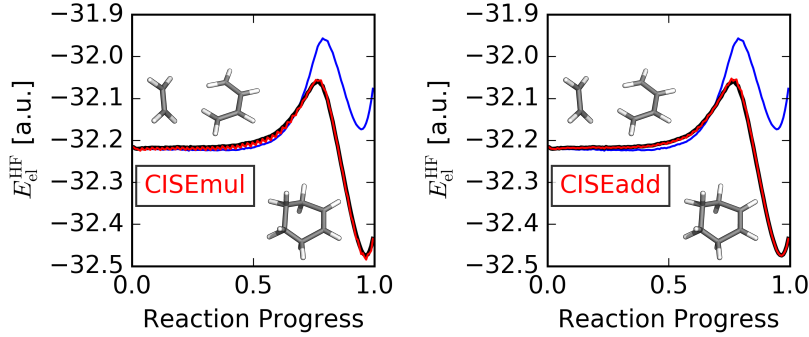


Figure 10: $E_{\text{el}}^{\text{HF}}$ for reaction A and the OM2-3G^{7-9,63} basis set (black line). $E_{\text{el}}^{\text{HF-NDDO}}$ with orbitals taken from the HF reference calculation and shifted by 2.1 a.u. (blue line). $E_{\text{el}}^{\text{HF-NDDO}}$ determined with the CISEmul approach (Eq. (31), red line left) and with the CISEadd approach (Eq. (32), red line right). The respective scaling matrices Γ , $\Gamma_{\mathbf{J}}$, and $\Gamma_{\mathbf{K}}$ are updated every third step.

error introduced by the NDDO approximation, we obtain large errors in the

absolute and relative $E_{\text{el}}^{\text{HF}}$. We would for example erroneously predict that cyclohexene is higher in energy than butadiene and ethylene (see the blue lines in Figure 10). When we apply the CISEmul approach, we see that we closely follow the exact $E_{\text{el}}^{\text{HF}}$. For reaction A, the CISEadd approach leads to smaller errors in general and to smoother reaction profiles (see Figure 10). In this example, we chose to update $\mathbf{\Gamma}^{\{\tilde{\mathbf{R}}_I^n\}}(\phi\mathbf{C})$ every third step. For this specific example, this leads to energies within chemical accuracy. Obviously, the update frequency is crucial when attempting to gain a maximal speed-up at a minimal loss of accuracy. One could imagine setting up a measure for the necessary update frequency for arbitrary reactions by exploiting structural similarity measures^{80,81} as demonstrated in Ref. 79.

Compared to other strategies which apply the NDDO approximation, the CISE approach has the advantage that we maintain complete error control on the resulting model because we can determine $\mathbf{\Gamma}^{\{\tilde{\mathbf{R}}_I^{(n+1)}\}}$ for a given molecule with nuclear coordinates $\{\tilde{\mathbf{R}}_I^{(n+1)}\}$ in case of doubt. In contrast to existing NDDO-SEMO models, we do not have to carry out any statistical calibration of parameters. Nevertheless, both correction approaches, the CISEmul and the CISEadd approach, suffer from limitations. The nuclear coordinates and also the density matrices obviously differ in a sequence of structures. Eqs. (31) and (32) will only yield sensible results when the change of both quantities remains small. We are currently exploring the possibility to apply this strategy in practice for sequences of structures as they occur during structure optimization, in Born–Oppenheimer molecular-dynamics trajectories, or in interactive reactivity studies.

6 Conclusions

The NDDO approximation is a central ingredient for many modern SEMO models. We studied the effect of the NDDO approximation on the ERIs in the symmetrically orthogonalized basis for the simplest possible model system, H_2 , and for a diverse set of molecules. As expected and in agreement with previous results,^{33–51} we found that the NDDO approximation leads

to significant errors for molecules in their equilibrium structure. The errors do only vanish in the atomization limit where the overlap between different basis functions vanishes. The errors in the ERIs in the symmetrically orthogonalized basis increase roughly linearly with the number of basis functions. Additionally, we found that the errors in the ERIs in the symmetrically orthogonalized basis depend strongly on the arrangement of the atomic nuclei. These nonnegligible errors introduced by NDDO may only be alleviated by an efficient error cancellation, which is in operation in SEMO models but not in HF theory. For HF calculations, error cancellation is unlikely to occur because of the fact that the ERIs in the symmetrically orthogonalized basis are contracted with elements of the density matrix.

We were then able to dissect how the NDDO approximation affects ERIs in the *molecular* orbital basis and, hence, correlation energies. We found that MP2 correlation energies are underestimated and the underestimation increases with the number of basis functions. This finding explains previous reports^{61,68} that correlation energies obtained with respect to an NDDO-SEMO reference wave function are far too small.

We proposed a local orthogonalization that allowed us to transgress the domain of minimal basis sets and to apply ordinary basis sets in conjunction with the NDDO approximation. While we observed a drastic reduction in the largest absolute errors in the ERIs in the symmetrically orthogonalized basis, we discovered another limitation of the NDDO approximation. Electronic energies calculated with the NDDO approximation do not converge with respect to the basis set size so that this solution to the small basis-set restriction of NDDO-SEMO models does not pay off.

We then continued to propose how one could still capitalize on the efficiency enabled by the NDDO approximation without significant loss of accuracy in a system-focused manner for similar structures which we called the correction inheritance to semiempirics (CISE) approach. Specifically, we proposed a strategy to correct for the errors introduced by the NDDO approximation in the two-electron matrices which was inspired by work of Roby and Sinanoğlu.³⁴ The two-electron matrix obtained within the NDDO approximation is modified with a correction matrix obtained from a refer-

ence HF, KS-DFT, or multi-configurational SCF calculation. These correction matrices are transferable to a certain degree within sequences of related structures.

Appendix: Computational Methodology

All calculations in this work were carried out with a modified version of PYSCF (version 1.4).^{82,83} The ERIs in the τ -basis were transformed to the corresponding ERIs in the χ -basis or in the ϕ -basis with the AO2MO integral transformation module of PYSCF. We applied the ECP-3G,^{7,63} STO-3G,⁸⁴ cc-pVXZ ($X = \text{D},$ ⁷⁰ $\text{T},$ ⁷⁰ $\text{Q},$ ⁷⁰ $5,$ ⁷⁰ 6 ⁷¹), and def2⁶⁴ basis sets in calculations.

Raymond and co-workers assembled a database considered to be representative of chemical space.⁶⁵ We randomly chose 5000 entries of the QM9 data set^{65,66} (set C) to study the error of the NDDO approximation across a large set of molecules. Additionally, we worked with linearly growing alkane chains (set B) with the stoichiometry $\text{C}_x\text{H}_{2x+2}$, ($x = 1, 2, \dots, 15$). We include the optimized structures as Supplementary Material. Finally, we selected three reactions (set D) which we had considered³¹ for interactive reactivity explorations in the framework of real-time quantum chemistry;^{27–32,85,86} they can be found in the Supplementary Material in Ref. 31.

Acknowledgements

This work was supported by the Schweizerischer Nationalfonds.

References

- [1] Pople, J. A.; Santry, D. P.; Segal, G. A. Approximate Self-Consistent Molecular Orbital Theory. I. Invariant Procedures, *J. Chem. Phys.* **1965**, *43*, 129–135.

- [2] Dewar, M. J. S.; Thiel, W. Ground States of Molecules. 38. The MNDO Method. Approximations and Parameters, *J. Am. Chem. Soc.* **1977**, *99*, 4899–4907.
- [3] Dewar, M. J. S.; Zoebisch, E. G.; Healy, E. F.; Stewart, J. J. P. Development and Use of Quantum Mechanical Molecular Models. 76. AM1: A New General Purpose Quantum Mechanical Molecular Model, *J. Am. Chem. Soc.* **1985**, *107*, 3902–3909.
- [4] Stewart, J. J. P. Optimization of Parameters for Semiempirical Methods I. Method, *J. Comput. Chem.* **1989**, *10*, 209–220.
- [5] Stewart, J. J. P. Optimization of Parameters for Semiempirical Methods V: Modification of NDDO Approximations and Application to 70 Elements, *J. Mol. Model.* **2007**, *13*, 1173–1213.
- [6] Stewart, J. J. P. Optimization of Parameters for Semiempirical Methods VI: More Modifications to the NDDO Approximations and Re-Optimization of Parameters, *J. Mol. Model.* **2012**, *19*, 1–32.
- [7] Kolb, M.; Thiel, W. Beyond the MNDO Model: Methodical Considerations and Numerical Results, *J. Comput. Chem.* **1993**, *14*, 775–789.
- [8] Weber, W.; Thiel, W. Orthogonalization Corrections for Semiempirical Methods, *Theor. Chem. Acc.* **2000**, *103*, 495–506.
- [9] Dral, P. O.; Wu, X.; Spörkel, L.; Koslowski, A.; Weber, W.; Steiger, R.; Scholten, M.; Thiel, W. Semiempirical Quantum-Chemical Orthogonalization-Corrected Methods: Theory, Implementation, and Parameters, *J. Chem. Theory Comput.* **2016**, *12*, 1082–1096.
- [10] Senn, H. M.; Thiel, W. QM/MM Methods for Biological Systems, *Top. Curr. Chem.* **2006**, *268*, 173–290.
- [11] Alexandrova, A. N.; Röthlisberger, D.; Baker, D.; Jorgensen, W. L. Catalytic Mechanism and Performance of Computationally Designed

- Enzymes for Kemp Elimination, *J. Am. Chem. Soc.* **2008**, *130*, 15907–15915.
- [12] Senn, H. M.; Thiel, W. QM/MM Methods for Biomolecular Systems, *Angew. Chem. Int. Ed.* **2009**, *48*, 1198–1229.
- [13] Alexandrova, A. N.; Jorgensen, W. L. Origin of the Activity Drop with the E50D Variant of Catalytic Antibody 34E4 for Kemp Elimination, *J. Phys. Chem. B* **2009**, *113*, 497–504.
- [14] Stewart, J. J. P. Application of the PM6 Method to Modeling Proteins, *J. Mol. Model.* **2009**, *15*, 765–805.
- [15] Acevedo, O.; Jorgensen, W. L. Advances in Quantum and Molecular Mechanical (QM/MM) Simulations for Organic and Enzymatic Reactions, *Acc. Chem. Res.* **2010**, *43*, 142–151.
- [16] Doron, D.; Major, D. T.; Kohen, A.; Thiel, W.; Wu, X. Hybrid Quantum and Classical Simulations of the Dihydrofolate Reductase Catalyzed Hydride Transfer Reaction on an Accurate Semi-Empirical Potential Energy Surface, *J. Chem. Theory Comput.* **2011**, *7*, 3420–3437.
- [17] Polyak, I.; Reetz, M. T.; Thiel, W. Quantum Mechanical/Molecular Mechanical Study on the Mechanism of the Enzymatic Baeyer–Villiger Reaction, *J. Am. Chem. Soc.* **2012**, *134*, 2732–2741.
- [18] Husch, T.; Yilmazer, N. D.; Balducci, A.; Korth, M. Large-Scale Virtual High-Throughput Screening for the Identification of New Battery Electrolyte Solvents: Computing Infrastructure and Collective Properties, *Phys. Chem. Chem. Phys.* **2015**, *17*, 3394–3401.
- [19] Husch, T.; Korth, M. Charting the Known Chemical Space for Non-Aqueous Lithium–air Battery Electrolyte Solvents, *Phys. Chem. Chem. Phys.* **2015**, *17*, 22596–22603.
- [20] Lepšík, M.; Řezáč, J.; Kolář, M.; Pecina, A.; Hobza, P.; Fanfrlík, J. The Semiempirical Quantum Mechanical Scoring Function for In Silico Drug Design, *ChemPlusChem* **2013**, *78*, 921–931.

- [21] Brahmshatriya, S. P.; Dobes, P.; Fanfrlik, J.; Rezac, J.; Paruch, K.; Bronowska, A.; Lepsík, M.; Hobza, P. Quantum Mechanical Scoring: Structural and Energetic Insights into Cyclin-Dependent Kinase 2 Inhibition by Pyrazolo[1,5-a]Pyrimidines, *Curr. Comput. Aided Drug Des.* **2013**, *9*, 118–129.
- [22] Yilmazer, N. D.; Korth, M. Enhanced Semiempirical QM Methods for Biomolecular Interactions, *Comput. Struct. Biotechnol. J.* **2015**, *13*, 169–175.
- [23] Vorlová, B.; Nachtigallová, D.; Jirásková-Vaníčková, J.; Ajani, H.; Jansa, P.; Řezáč, J.; Fanfrlík, J.; Otyepka, M.; Hobza, P.; Konvalinka, J.; Lepšík, M. Malonate-Based Inhibitors of Mammalian Serine Racemase: Kinetic Characterization and Structure-Based Computational Study, *Eur. J. Med. Chem.* **2015**, *89*, 189–197.
- [24] Yilmazer, N. D.; Korth, M. Prospects of Applying Enhanced Semi-Empirical QM Methods for Virtual Drug Design, *Curr. Med. Chem.* **2016**, *23*, 2101–2111.
- [25] Sulimov, A. V.; Kutov, D. C.; Katkova, E. V.; Ilin, I. S.; Sulimov, V. B. New generation of docking programs: Supercomputer validation of force fields and quantum-chemical methods for docking, *J. Mol. Graph. Model.* **2017**, *78*, 139–147.
- [26] Bosson, M.; Richard, C.; Plet, A.; Grudinin, S.; Redon, S. Interactive quantum chemistry: A divide-and-conquer ASED-MO method, *J. Comput. Chem.* **2012**, *33*, 779–790.
- [27] Haag, M. P.; Reiher, M. Real-Time Quantum Chemistry, *Int. J. Quantum Chem.* **2013**, *113*, 8–20.
- [28] Haag, M. P.; Vaucher, A. C.; Bosson, M.; Redon, S.; Reiher, M. Interactive Chemical Reactivity Exploration, *ChemPhysChem* **2014**, *15*, 3301–3319.

- [29] Haag, M. P.; Reiher, M. Studying chemical reactivity in a virtual environment, *Faraday Discuss.* **2014**, *169*, 89–118.
- [30] Vaucher, A. C.; Haag, M. P.; Reiher, M. Real-Time Feedback from Iterative Electronic Structure Calculations, *J. Comput. Chem.* **2016**, *37*, 805–812.
- [31] Mühlbach, A. H.; Vaucher, A. C.; Reiher, M. Accelerating Wave Function Convergence in Interactive Quantum Chemical Reactivity Studies, *J. Chem. Theory Comput.* **2016**, *12*, 1228–1235.
- [32] Heuer, M. A.; Vaucher, A. C.; Haag, M. P.; Reiher, M. Integrated Reaction Path Processing from Sampled Structure Sequences, *J. Chem. Theory Comput.* **2018**, *14*, 2052–2062.
- [33] Cook, D. B.; Hollis, P. C.; McWeeny, R. Approximate Ab Initio Calculations on Polyatomic Molecules, *Mol. Phys.* **1967**, *13*, 553–571.
- [34] Roby, K. R.; Sinanoğlu, O. On the Performance and Parameter Problems of Approximate Molecular Orbital Theory, with Comparative Calculations on the Carbon Monoxide Molecule, *Int. J. Quantum Chem.* **1969**, *3*, 223–236.
- [35] Sustmann, R.; Williams, J. E.; Dewar, M. J. S.; Allen, L. C.; von Rague Schleyer, P. Molecular Orbital Calculations on Carbonium Ions. II. Methyl, Ethyl, and Vinyl Cations. The Series $C_3H_7^+$, *J. Am. Chem. Soc.* **1969**, *91*, 5350–5357.
- [36] Gray, N. A. B.; Stone, A. J. Justifiability of the ZDO approximation in terms of a power series expansion, *Theor. Chim. Acta* **1970**, *18*, 389–390.
- [37] Roby, K. R. On the Justifiability of Neglect of Differential Overlap Molecular Orbital Methods, *Chem. Phys. Lett.* **1971**, *11*, 6–10.
- [38] Brown, R. D.; Burden, F. R.; Williams, G. R.; Phillips, L. F. Simplified Ab-Initio Calculations on Hydrogen-Containing Molecules, *Theor. Chim. Acta* **1971**, *21*, 205–210.

- [39] Roby, K. R. Fundamentals of an Orthonormal Basis Set Molecular Orbital Theory, *Chem. Phys. Lett.* **1972**, 12, 579–582.
- [40] Brown, R. D.; Burton, P. G. ‘Balance’ and Predictive Capability in Approximate Molecular Orbital Theory, *Chem. Phys. Lett.* **1973**, 20, 45–49.
- [41] Birner, P.; Köhler, H. J.; Weiss, C. C–H Acidity Comparative CNDO/2 and NDDO Calculations on the Reactivity of Azabenzenes, *Chem. Phys. Lett.* **1974**, 27, 347–350.
- [42] Chandler, G. S.; Grader, F. E. A Re-Examination of the Justification of Neglect of Differential Overlap Approximations in Terms of a Power Series Expansion in S, *Theor. Chim. Acta* **1980**, 54, 131–144.
- [43] Duke, B. J.; Collins, M. P. S. The Ab Initio Neglect of Differential Diatomic Overlap Method, *Theor. Chim. Acta* **1981**, 58, 233–244.
- [44] Weinhold, F.; Carpenter, J. E. A Collection of Papers Presented at the First World Congress of Theoretical Chemists: Some Remarks on Nonorthogonal Orbitals in Quantum Chemistry, *J. Mol. Struct. Theochem* **1988**, 165, 189–202.
- [45] Koch, W. Neglect of Diatomic Differential Overlap (NDDO) in Non-Empirical Quantum Chemical Orbital Theories, *Z. Naturforsch. A* **1993**, 48, 819–828.
- [46] Neymeyr, K.; Seelig, F. F. “Neglect of Diatomic Differential Overlap” in Nonempirical Quantum Chemical Orbital Theories. I. On the Justification of the Neglect of Diatomic Differential Overlap Approximation, *Int. J. Quantum Chem.* **1995**, 53, 515–518.
- [47] Neymeyr, K.; Seelig, F. F. “Neglect of Diatomic Differential Overlap” in Nonempirical Quantum Chemical Orbital Theories. II. A Polynomial Expansion for $\Delta^{-1/2}$ in Terms of Legendre and Chebyshev Polynomials, *Int. J. Quantum Chem.* **1995**, 53, 519–535.

- [48] Neymeyr, K.; Engel, K. “Neglect of Diatomic Differential Overlap” in Nonempirical Quantum Chemical Orbital Theories. III. On the Spectrum of the Overlap Matrix for Diatomic Molecules over Locally Orthogonalized Basis Functions, *Int. J. Quantum Chem.* **1995**, *53*, 537–540.
- [49] Neymeyr, K. “Neglect of Diatomic Differential Overlap” in Nonempirical Quantum Chemical Orbital Theories. IV. An Examination of the Justification of the Neglect of Diatomic Differential Overlap (NDDO) Approximation, *Int. J. Quantum Chem.* **1995**, *53*, 541–552.
- [50] Neymeyr, K. “Neglect of Diatomic Differential Overlap” in Nonempirical Quantum Chemical Orbital Theories. V. A Calculus of Error Concerning the Justification of the Neglect of Diatomic Differential Overlap (NDDO) Approximation, *Int. J. Quantum Chem.* **1995**, *53*, 553–568.
- [51] Tu, Y.; Jacobsson, S. P.; Laaksonen, A. Re-examination of the NDDO approximation and introduction of a new model beyond it, *Mol. Phys.* **2003**, *101*, 3009–3015.
- [52] Husch, T.; Vaucher, A. C.; Reiher, M. Semiempirical Molecular Orbital Models based on the Neglect of Diatomic Differential Overlap Approximation, *Int. J. Quantum Chem.* **2018**, accepted, [arXiv: 1806.06147].
- [53] Giese, T. J.; York, D. M. Improvement of Semiempirical Response Properties with Charge-Dependent Response Density, *J. Chem. Phys.* **2005**, *123*, 164108.
- [54] Szabo, A.; Ostlund, N. S. *Modern Quantum Chemistry: Introduction to Advanced Electronic Structure Theory*; Dover Publications: New York, 1996.
- [55] Helgaker, T.; Jorgensen, P.; Olsen, J. *Molecular Electronic-Structure Theory*; John Wiley & Sons: Chichester, 2012.
- [56] Kołos, W. Possible Improvements of the Interaction Energy Calculated Using Minimal Basis Sets, *Theor. Chim. Acta* **1979**, *51*, 219–240.

- [57] Francl, M. M.; Pietro, W. J.; Hehre, W. J.; Binkley, J. S.; Gordon, M. S.; DeFrees, D. J.; Pople, J. A. Self-consistent Molecular Orbital Methods. XXIII. A Polarization-type Basis Set for Second-row Elements, *J. Chem. Phys.* **1982**, 77, 3654–3665.
- [58] Davidson, E. R.; Feller, D. Basis Set Selection for Molecular Calculations, *Chem. Rev.* **1986**, 86, 681–696.
- [59] Dewar, M. J. S. The Semiempirical Approach to Chemistry, *Int. J. Quantum Chem.* **1992**, 44, 427–447.
- [60] Thiel, W. Semiempirical NDDO Calculations with STO-3G and 4-31G Basis Sets, *Theor. Chim. Acta* **1981**, 59, 191–208.
- [61] Gleghorn, J. T.; McConkey, F. W. Extended Basis NDDO Calculations on Diatomic Molecules, *Theor. Chim. Acta* **1982**, 61, 283–293.
- [62] Löwdin, P.-O. On the Nonorthogonality Problem, *Adv. Quantum Chem.* **1970**, 5, 185–199.
- [63] Stevens, W. J.; Basch, H.; Krauss, M. Compact Effective Potentials and Efficient Shared-exponent Basis Sets for the First- and Second-row Atoms, *J. Chem. Phys.* **1984**, 81, 6026–6033.
- [64] Weigend, F.; Ahlrichs, R. Balanced basis sets of split valence, triple zeta valence and quadruple zeta valence quality for H to Rn: Design and assessment of accuracy, *Phys. Chem. Chem. Phys.* **2005**, 7, 3297–3305.
- [65] Ruddigkeit, L.; van Deursen, R.; Blum, L. C.; Reymond, J.-L. Enumeration of 166 billion organic small molecules in the chemical universe database GDB-17, *J. Chem. Inf. Model.* **2012**, 52, 2864–2875.
- [66] Ramakrishnan, R.; Dral, P. O.; Rupp, M.; von Lilienfeld, O. A. Quantum chemistry structures and properties of 134 kilo molecules, *Sci. Data* **2014**, 1, 140022.

- [67] Koster, J. L.; Ruttink, P. J. A. Non-empirical approximate calculations for the ground states of H_2 and H_3 including complete configuration interactions, *Chem. Phys. Lett.* **1972**, *17*, 419–421.
- [68] Thiel, W. The MNDOC Method, a Correlated Version of the MNDO Model, *J. Am. Chem. Soc.* **1981**, *103*, 1413–1420.
- [69] Clark, T.; Chandrasekhar, J. NDDO-Based CI Methods for the Prediction of Electronic Spectra and Sum-Over-States Molecular Hyperpolarization, *Isr. J. Chem.* **1993**, *33*, 435–448.
- [70] Dunning Jr., T. H. Gaussian basis sets for use in correlated molecular calculations. I. The atoms boron through neon and hydrogen, *J. Chem. Phys.* **1989**, *90*, 1007–1023.
- [71] Peterson, K. A.; Woon, D. E.; Dunning Jr, T. H.; to be published, <https://bse.pnl.gov/bse/portal> (Accessed: 01. August 2018).
- [72] Jensen, F. The basis set convergence of the Hartree–Fock energy for H_2 , *J. Chem. Phys.* **1999**, *110*, 6601–6605.
- [73] Kollmar, C.; Böhm, M. C. An Analysis of the Zero Differential Overlap Approximation. Towards an Improved Semiempirical MO Method beyond It, *Theor. Chim. Acta* **1995**, *92*, 13–47.
- [74] Dewar, M. J. S.; Thiel, W. A Semiempirical Model for the Two-Center Repulsion Integrals in the NDDO Approximation, *Theor. Chim. Acta* **1976**, *46*, 89–104.
- [75] Korth, M.; Thiel, W. Benchmarking Semiempirical Methods for Thermochemistry, Kinetics, and Noncovalent Interactions: OMx Methods Are Almost As Accurate and Robust As DFT-GGA Methods for Organic Molecules, *J. Chem. Theory Comput.* **2011**, *7*, 2929–2936.
- [76] Dral, P. O.; Wu, X.; Spörkel, L.; Koslowski, A.; Thiel, W. Semiempirical Quantum-Chemical Orthogonalization-Corrected Methods: Benchmarks for Ground-State Properties, *J. Chem. Theory Comput.* **2016**, *12*, 1097–1120.

- [77] Margraf, J. T.; Claudino, D.; Bartlett, R. J. Determination of Consistent Semiempirical One-Centre Integrals Based on Coupled-Cluster Theory, *Mol. Phys.* **2017**, *115*, 538–544.
- [78] Simm, G. N.; Reiher, M. Systematic Error Estimation for Chemical Reaction Energies, *J. Chem. Theory Comput.* **2016**, *12*, 2762–2773.
- [79] Simm, G.; Reiher, M. Error-Controlled Exploration of Chemical Reaction Networks with Gaussian Processes, *J. Chem. Theory Comput.* **2018**, submitted, [arXiv: 1805.09886].
- [80] De, S.; Bartók, A. P.; Csányi, G.; Ceriotti, M. Comparing Molecules and Solids across Structural and Alchemical Space, *Phys. Chem. Chem. Phys.* **2016**, *18*, 13754–13769.
- [81] Huang, B.; von Lilienfeld, O. A. Understanding molecular representations in machine learning: The role of uniqueness and target similarity, *J. Chem. Phys.* **2016**, *145*, 161102.
- [82] Sun, Q.; Berkelbach, T. C.; Blunt, N. S.; Booth, G. H.; Guo, S.; Li, Z.; Liu, J.; McClain, J. D.; Sayfutyarova, E. R.; Sharma, S.; Wouters, S.; Chan, G. K.-L. PySCF: the Python-based simulations of chemistry framework, *WIREs Comput. Mol. Sci* **2017**, *8*, e1340.
- [83] Sun, Q. Libcint: An efficient general integral library for Gaussian basis functions, *J. Comput. Chem.* **2015**, *36*, 1664–1671.
- [84] Hehre, W. J.; Stewart, R. F.; Pople, J. A. Self-Consistent Molecular-Orbital Methods. I. Use of Gaussian Expansions of Slater-Type Atomic Orbitals, *J. Chem. Phys.* **1969**, *51*, 2657–2664.
- [85] Marti, K. H.; Reiher, M. Haptic quantum chemistry, *J. Comput. Chem.* **2009**, *30*, 2010–2020.
- [86] Haag, M. P.; Marti, K. H.; Reiher, M. Generation of Potential Energy Surfaces in High Dimensions and Their Haptic Exploration, *ChemPhysChem* **2011**, *12*, 3204–3213.